JOURNAL OF Applied Polymer SCIENCE

Efficient removal of Cu(II) using amino-functionalized superparamagnetic nanoparticles prepared via SI-ATRP

Caideng Yuan,[1] Mingtong Cui,[1] Longlong Feng,[1,2] Jingpeng Wang,[1] Yan Peng[1]

[1]Department of Polymer Science and Engineering, School of Chemical Engineering and Technology, Tianjin University, Tianjin 300072, China

[2]Tianjin Binhai Foreign Language School, Binhai New Area, Tianjin 300450, China

Group Authorship Information: All the authors listed in the manuscript have substantial contributions to this study. The research was designed by Caideng Yuan and Mingtong Cui and then revised by Longlong Feng, Jingpeng Wang and Yan Peng. The experiments were carried out and the obtained data were analyzed by Mingtong Cui and Longlong Feng, with the assistance of Jingpeng Wang. After the manuscript was drafted by Mingtong Cui, it was revised critically by Caideng Yuan and Yan Peng. All the authors approve the submitted and final versions of the paper.

Correspondence to: C. Yuan (E-mail: cdyuan@tju.edu.cn)

ABSTRACT: An amino-functionalized nano-adsorbent (DETA-MNPs) was prepared by a process involving: (1) synthesis of superparamagnetic Fe_3O_4 nanoparticles; (2) introduction of amino groups after which ATRP initiator was anchored; (3) grafting of glycidyl methacrylate (GMA) via SI-ATRP; and (4) ring-opening reaction of epoxy groups with diethylenetriamine (DETA). The nano-adsorbent was characterized by Fourier transform infrared spectroscopy (FT-IR), X-ray diffraction (XRD), transmission electron microscope (TEM), and vibrating sample magnetometer (VSM) and applied to remove Cu(II) in batch experiments. The effects of pH, Cu(II) concentrations, solution ionic strength, and contact time were investigated. The results show that the DETA-MNPs are spherical with cubic spine structure, high saturation magnetization (41.9 emu g^{-1}), and an average diameter of 10 nm. The maximum Cu(II) adsorption capacity achieves 83.33 mg g^{-1} at pH 5.0 by Langmuir model. The adsorption process is highly pH-dependent and reaches equilibrium within 20 min. Furthermore, the DETA-MNPs exhibit excellent dispersibility and reusability.
 J. Appl. Polym. Sci. **2016**, *133*, 42859.

KEYWORDS: adsorption; applications; functionalization of polymers; nanoparticles; nanowires and nanocrystals; properties and characterization

Received 30 April 2015; accepted 18 August 2015

DOI: 10.1002/app.42859

INTRODUCTION

As one of the top-priority contaminants, copper is often introduced into natural water via effluents from a variety of industries such as petroleum refining, chemical manufacturing, metallurgical mining, electro-plating, medication, fertilizer industry, and dye wastewater.[1,2] Its high toxicity to both the environment and living organisms even at relatively low concentrations[3,4] has attracted more researchers to remove it from waste water. Several conventional methods are applied to remove Cu(II) from wastewater like ion exchange, solvent extraction, electrodialysis and filtration, adsorption, chemical reduction, and precipitation,[5–9] among which adsorption has been receiving considerable attention for its high efficiency, good controllability, and relatively low cost. Up to now, various of adsorbents, such as activated carbons, clay minerals, biomaterials, and functionalized polymers,[10–14] are investigated for Cu(II) removal, yet none is perfect. Thus, it's still urgent to develop an effective, economical, and easy-to-separate adsorbent to meet the strict standard.

It was reported that magnetic nanoparticles (MNPs) modified by amino groups are of excellent performance in adsorbing and trapping Cu(II) due to the high affinity of Cu(II) and amino groups on the adsorbent.[15,16] Different nitrogen compounds such as diethylenetriamine (DETA),[17,18] tetraethylenepentamine (TEPA),[19] 3-aminpropyltriethoxysilane (APTES),[20] 1,6-hexadiamine,[21] ethylenediaminetetraacetic acid (EDTA),[22,23] polydopamine (PDA),[24] poly(allylamine hydrochloride) (PAH),[25] and 1,2-cyclohexylenedinitrilotetraacetic acid (CDTA)[26] are applied to synthesize amino-functionalized nanoparticles for Cu(II) removal and chemical modification via grafting of reactive polymers is proved to be an efficient approach to functionalize the surface of particles.[27,28] However, the content of amino groups anchored on the surface of nanoparticles synthesized by the conventional modification process is unpredictable.

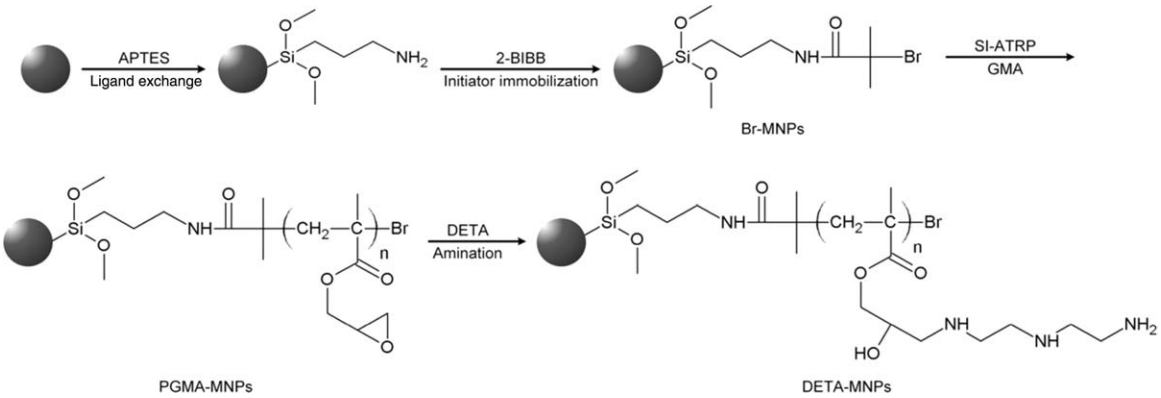

Figure 1. Synthesis route of DETA-MNPs.

To solve the problem, surface-initiated atom transfer radical polymerization (SI-ATRP) is applied to realizing the modification process in a controlled/living manner.[29] In this work, amino-functionalized superparamagnetic nanoparticles were prepared by grafting poly (glycidyl methacrylate) (PGMA) brushes onto the surface of MNPs via SI-ATRP and then aminated by DETA through ring-opening reaction. The synthetic process of DETA-modified magnetic nanoparticles (DETA-MNPs) is shown in Figure 1. The fabricated materials were characterized by various techniques including Fourier transform infrared spectroscopy (FT-IR), X-ray diffraction (XRD), transmission electron microscope (TEM), and vibrating sample magnetometer (VSM). Cu(II) was chosen to test the adsorption ability of DETA-MNPs in batch experiments. The effects of pH, Cu(II) concentrations, solution ionic strength, and contact time on the adsorption efficiency were investigated to determine the optimal adsorption conditions. Furthermore, the adsorption/desorption cycles were executed to evaluate the reusability of the adsorbents. The results show that DETA-MNPs are promising adsorbents for Cu(II) removal.

EXPERIMENTAL

Materials

$FeCl_3{\cdot}6H_2O$, $FeCl_2{\cdot}4H_2O$, oleic acid, tetrahydrofuran (THF), DETA, copper(I)-bromide (CuBr), and 2,2′-bipyridine (Bpy) were of analytical grade and purchased from Tianjin Guangfu Fine Chemical Research Institute (Tianjin, China). Glycidyl methacrylate (GMA, 97%), 3-aminopropyltriethoxysilane (APTES, 98%), and 2-bromoisobutyryl bromide (2-BIBB, 98%) were obtained from Aladdin Chemistry (Shanghai, China). Toluene, triethylamine (TEA), and dichloromethane were analytical reagents and supplied by Tianjin Jiangtian Chemical Reagent (Tianjin, China). Prior to use, toluene, TEA, and dichloromethane were purified by distillation in the presence of CaH_2. GMA was used after the removal of the inhibitors. Milli-Q water was redeionized (specific conductance $< 0.1\ \mu S\ cm^{-1}$) and deoxygenated by bubbling N_2 gas for 1.5 h. All the other reagents were used as received.

Fabrication of DETA-MNPs

Preparation of Oleic Acid Coated MNPs (OA-MNPs). First, a known quantity of $FeCl_3{\cdot}6H_2O$, $FeCl_2{\cdot}4H_2O$, and oleic acid was dissolved in a solvent mixture (25 mL ethanol and 100 mL Milli-Q water) which is oxygen free under vigorous mechanical stirring to form a homogeneous solution. Next, NaOH solution was added quickly and the solution was maintained at 70°C for 1 h before 1.0*M* HCl was applied to adjust the solution pH to 2.0–3.0. Then, the nanoparticles were separated using a permanent magnet and washed with Milli-Q water for five times. Finally, the resultant was washed with ethanol to remove the physically adsorbed oleic acid and dried for 12 h at 55°C so that the product OA-MNPs were obtained.

Synthesis of Initiator-Immobilized MNPs. Synthesis of the initiator-immobilized MNPs was performed using a method similar to that reported by Liu *et al.*[30] In brief, 2.02 g of OA-MNPs were first dispersed in 50 mL of toluene. After sonication for 10 min, 6.8 mL of APTES was added dropwise and the reaction was lasted for 6 h at room temperature under vigorous stirring. The APTES-coated MNPs (APTES-MNPs) were washed with ethanol (4 × 15 mL) and dichloromethane (4 × 15 mL) so that the unreacted APTES was removed. The resultant was separated by an external magnetic field and dried for 12 h at 35°C to yield dried APTES-MNPs for immobilizing the ATRP initiator.

The initiator immobilization procedure was carried out as follows: 1.83 g of APTES-MNPs were mixed with 30 mL of dichloromethane and 2.4 mL of TEA and stirred for 40 min at 0°C followed by the addition of 2.4 mL of 2-BIBB. After the solution was mechanically stirred for 12 h, the resultant was centrifuged and washed with water-alcohol mixture to remove the residue initiator. The Br-MNPs were subsequently washed with acetone and dried for 24 h at room temperature.

Grafting PGMA Brushes onto MNPs via SI-ATRP. About 0.5 g of Br-MNPs, 2.0 g of GMA, and 10 mL of THF were added into a 50-mL flask and then sonicated to form a brown solution. After that, 20.4 mg of CuBr and 66.4 mg of Bpy were added. Then, the flask was sealed and kept at 35°C to allow reaction. The reaction time (2, 4, 6, 8, and 10 h) was investigated to determine the optimal SI-ATRP time. The mixture was diluted with THF and centrifuged (4000 rpm, 8 min) to remove the Cu(II) ions generated in the SI-ATRP process. Next, ethanol was used to precipitate the nanoparticles which were redispersed in THF and centrifuged (2000 rpm, 8 min) to remove the remaining Cu(II) ions. At last, PGMA-MNPs were washed with ethanol for five times and dried for 12 h at 45°C.

Modification of MNPs with DETA. Nearly 10 mL of THF containing 0.25 g of PGMA-MNPs was added into a 50-mL flask together with 5 mL of DETA. The mixture was maintained at 80°C, pH 11.0 (adjusted with NaOH) for 10 h under mechanical stirring. Then, the resultant was washed with acetone and Milli-Q water by turns to remove excess DETA. The DETA-MNPs were dried for the further study.

It's of vital importance that N_2 gas was purged during all the synthesis operations to avoid oxygen contamination.

Characterization

The amount of PGMA grafted onto the nanoparticles via SI-ATRP reaction was examined. The grafting density is calculated by the following equation:

$$\mathrm{GD}(\%) = \frac{W_a - W_b}{W_b} \times 100\% \quad (1)$$

where W_b and W_a are the weights of the Br-MNPs before and after grafting, respectively.

For determining the bromine content of Br-MNPs, 0.2 g of Br-MNPs were first dissolved into 10 mL of 5.0*M* NaOH solution in ethanolic and refluxed for 3 h. Then, the nanoparticles was separated from the mixture and washed with Milli-Q water for three times. Finally, the solution was diluted to 250 mL with Milli-Q water and the NaBr content was determined by mercuric thiocyanate spectrophotometric method according to the standard HJ/T 27-1999.[31] The bromine content of Br-MNPs equals to that of NaBr.

The available amino content of DETA-MNPs was confirmed as follows.[32] Nearly 0.2 g of DETA-MNPs was dispersed in 10 mL Milli-Q water in a conical flask. After 24 h, 10 mL of 2.0*M* HCl solution was added into the mixture and shaken for another 1 h. Then, the nanoparticles were separated and HCl concentration was determined by titration with 2.0*M* NaOH solution, thus the available amino content of DETA-MNPs was calculated from the HCl concentration.

The content of epoxy group of PGMA-MNPs was measured by acetone-hydrochloride method[33] according to the standard GB/T 1677-2008 as follows. 0.5 g of PGMA-MNPs was dispersed in 20 mL acetone-hydrochloride solution and kept in dark place for 30 min. After that, mixed indicators were added and the available epoxy groups were determined by titration with 0.15*M* NaOH solution.

The adsorption capacity is calculated by the following equation:

$$q_e = \frac{C_o - C_e}{m} V \quad (2)$$

where q_e (mg g^{-1}) is the amount of Cu(II) adsorbed on the adsorbent. C_o (mg L^{-1}) and C_e (mg L^{-1}) are the initial and equilibrium concentrations of Cu(II) in the aqueous solution, respectively. V (L) is the volume of the solution and m (g) is the adsorbent dosage.

To confirm the synthesis of DETA-MNPs, FT-IR spectra were collected in 4000–500 cm^{-1} using a Thermo Nicolet instrument (NICOLET380, Thermo Electron, USA). XRD patterns were recorded using Co Kα irradiation on X'pert pro (PANalytical, Netherlands) at a scan speed of 4° min^{-1}. The morphology of the composites was studied with transmission electron microscope (TEM, JEM-2100F, Hirata, Japan). The magnetic properties were obtained from a vibrating sample magnetometer (VSM, LDJ 9600-1, USA) at room temperature. Inductively Coupled Plasma Optical Emission Spectroscopy (ICP-OES, Vista-MPX, Varian, USA) was applied to determine the concentrations of Cu(II) after adsorption.

Adsorption Experiments

All the adsorption experiments were conducted at 25°C on a constant temperature shaking table (SHK-99-II, Beijing North TZ-Biotech Develop, Beijing, China). The standard solution of Cu(II) (1000 mg L^{-1}) was prepared by dissolving a known quantity of $Cu(NO_3)_2$ in Milli-Q water and kept in dark place at 4°C prior to use. The standard solution was diluted to desired concentrations and the pH of the solutions was adjusted with 0.1*M* HNO_3 or 0.1*M* NaOH solution.

The effects of initial solution pH (2.0–6.5), concentration (50–200 mg L^{-1}), contact time (0–100 min), and the solution ionic strength (0–0.05*M*) on the adsorption capacity were investigated through batch adsorption experiments. The adsorption experiments with initial concentration of Cu(II) ions ranging from 50 to 200 mg L^{-1} were carried out to determine the adsorption isotherm, which is important to estimate the maximum adsorption capacity of the adsorbents. The effect of the initial solution pH on adsorption capacity was investigated in the pH range of 2.0–6.5 with different Cu(II) concentrations (50, 100, and 200 mg L^{-1}) at 25°C. The experiments lasted for 100 min to ensure adsorption equilibrium was reached. Experiments to study the influence of the solution ionic strength ($NaNO_3$, 0–0.05 M) and the contact time (0–100 min) on the equilibrium adsorption capacity were conducted at 25°C, pH = 5.0. Consecutive adsorption/desorption cycles were repeated six times in order to evaluate the reusability of the adsorbents using the same nanoparticles. The Cu(II) desorption was performed in 0.1*M* HNO_3 solution for 1 h at 25°C. After each cycle, the adsorbents were washed with Milli-Q water to neutrality for removing the excess HNO_3. After adsorption, the suspensions were filtered through a 0.45-μm polyethersulfone membrane and the filtrates were suitably pretreated and then analyzed Cu(II) concentration by means of ICP-OES.

RESULTS AND DISCUSSION

Preparation and Characterization of DETA-MNPs

The synthesis route of DETA-MNPs is presented in Figure 1. First, OA-MNPs were obtained by an improved coprecipitation method using oleic acid as surfactant. Second, OA-MNPs were modified with APTES through ligand exchange to introduce amino groups, with which 2-BIBB reacted to yield the ATRP initiator, i.e. Br-MNPs. Third, PGMA brushes were grafted onto the surface of the nanoparticles via a SI-ATRP reaction to produce a high density of epoxy groups. Finally, abundant amino groups were anchored through the ring-opening reaction between the epoxy groups of PGMA-MNPs and DETA.

The optimal time for SI-ATRP reaction is determined according to the amount of PGMA grafted onto the nanoparticles. It is found that the grafting density linearly goes up to 102% with the SI-ATRP time prolonging to 6 h and then slows down afterward. The possible explanation is the increasing viscosity as the reaction proceeds.

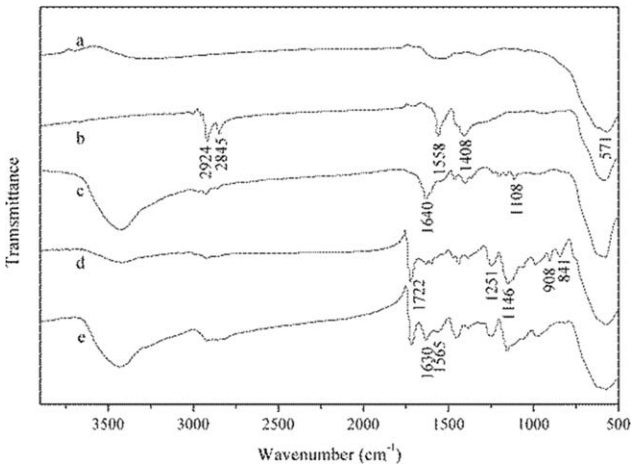

Figure 2. FT-IR spectra of (a) MNPs, (b) OA-MNPs, (c) Br-MNPs, (d) PGMA-MNPs, and (e) DETA-MNPs.

What's more, the homopolymerization of PGMA may have prevented the diffusion of GMA monomer on the nanoparticles surface.[34] Thus, the SI-ATRP reaction time was set at 6 h.

The available bromine content of Br-MNPs is calculated from the mercuric thiocyanate spectrophotometric method to be 0.39 mmol g^{-1} while the available amino content of DETA-MNPs is 3.13 mmol g^{-1}. The amount of epoxy groups of PGMA-MNPs is determined by acetone-hydrochloride method to be 3.42 mmol g^{-1}. Moreover, the grafting density obtained at 6 h indicates that the GMA content of PGMA-MNPs is 3.56 mmol g^{-1}. Taken the bromine content (0.39 mmol g^{-1}) into account, the average degree of polymerization per initiation site is estimated to be 9. These results reveal that PGMA with different average polymerization degree can be created for specific application by controlling the SI-ATRP reaction time.

The FT-IR spectra of (a) MNPs, (b) OA-MNPs, (c) Br-MNPs, (d) PGMA-MNPs, and (e) DETA-MNPs are shown in Figure 2. The bands at around 571 cm^{-1} belong to Fe—O stretching vibration. OA-MNPs are confirmed by the peaks at 1408 and 1508 cm^{-1} which are assigned to COO^- group and those at 2924 and 2845 cm^{-1}, which are assigned to C═H stretching vibration.[35] The characteristic peaks of Si—O—Si group at around 1108 cm^{-1} as well as N—C═O groups at 1640 cm^{-1} indicate that APTES is grafted on the surface of OA-MNPs.[30] New bands at 908 and 841 cm^{-1} (epoxy groups), 1146 and 1251 cm^{-1} (C—O—C) and 1720 cm^{-1} (C═O) imply that PGMA brushes are grafted onto the nanoparticles.[30,36] The characteristic peaks at 1630 and 1565 cm^{-1} correspond to the vibrations of $-NH_2$ and —NH groups,[37] which demonstrate that DETA-MNPs are successfully prepared.

The XRD patterns of (a) OA-MNPs and (b) DETA-MNPs are shown in Figure 3. The six typical peaks (2θ = 35.22, 41.49, 50.63,

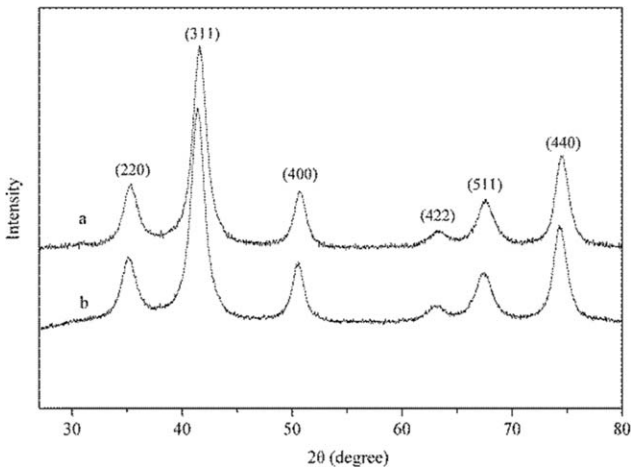

Figure 3. XRD patterns of (a) OA-MNPs and (b) DETA-MNPs.

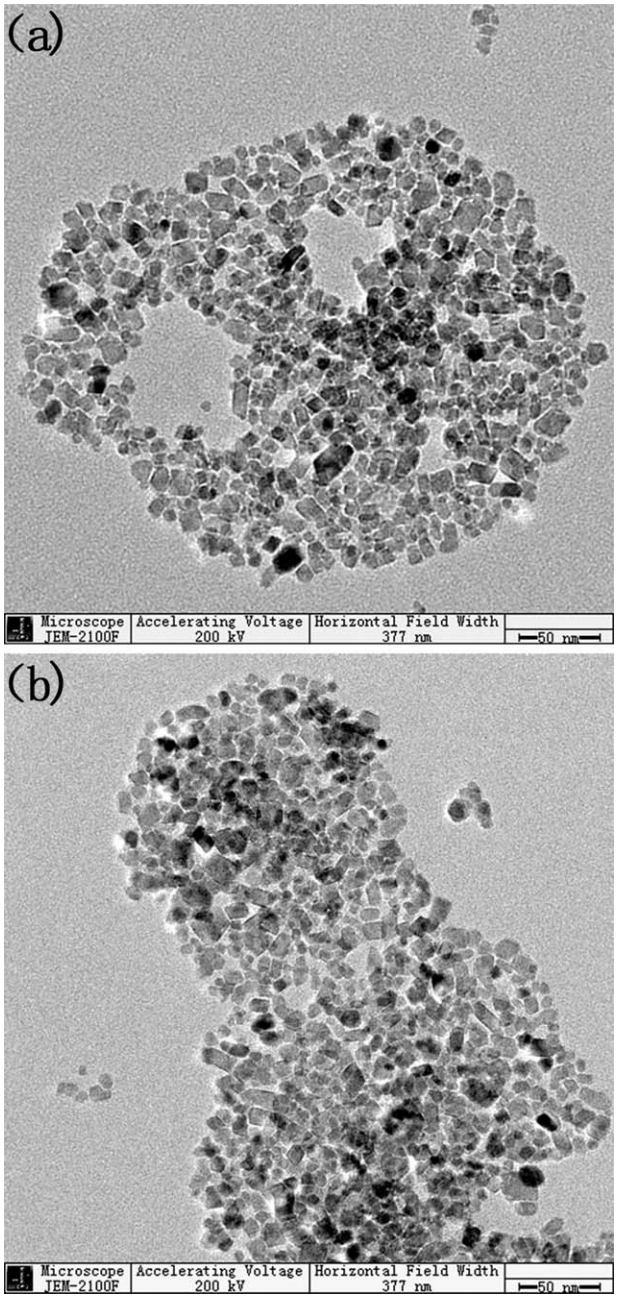

Figure 4. TEM micrographs of (a) OA-MNPs dispersed in hexane and (b) DETA-MNPs dispersed in Milli-Q water.

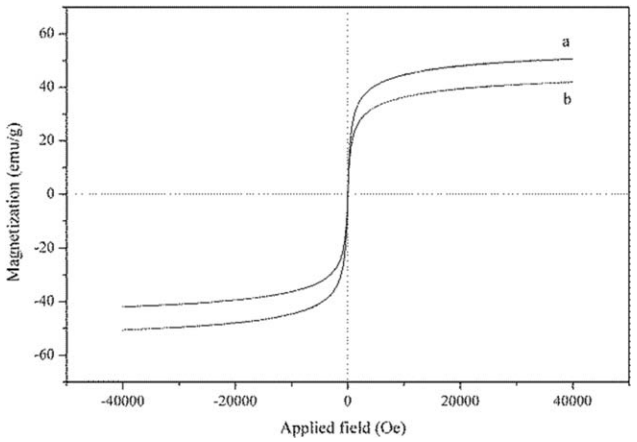

Figure 5. Magnetic hysteresis loop of (a) OA-MNPs and (b) DETA-MNPs at room temperature.

63.20, 67.51, 74.45), marked by their indices [(220), (311), (400), (422), (511), and (440)] in accordance with the database (JCPDS 01-1111), are observed, implying the nanoparticles are all with cubic spine structure[38] and the modification process does not result in the phase change of Fe_3O_4. In addition, the core diameter of the nanoparticles is calculated from Scherrer's equation to be around 10 nm, which is in accordance with that obtained from the TEM micrographs.

Figure 4 shows the typical TEM micrographs of (a) OA-MNPs and (b) DETA-MNPs. As shown in the figure, the nanoparticles are spherical with uniform size. Both the average diameters of the OA-MNPs and DETA-MNPs are ~10 nm. The OA-MNPs can be well dispersed in organic solvent such as hexane and toluene but not in Milli-Q water due to the presence of surfactant on the surface. On the other hand, the DETA-MNPs disperse better in aqueous solutions and no precipitation phenomenon is observed even after several months.

The magnetic properties of OA-MNPs and DETA-MNPs were measured by VSM at room temperature. As shown in Figure 5, the saturation magnetization of OA-MNPs and DETA-MNPs are 50.6 and 41.9 emu g^{-1}, respectively. The difference may be attributed to the decrease of Fe_3O_4 content resulting from immobilization of the nanoparticles. In addition, the reversible hysteresis and zero coercivity indicate the nanoparticles are superparamagnetic at room temperature. Therefore, the nano-adsorbents can be easily separated from aqueous solutions.

The dispersibility and magnetic sensitivity of the DETA-MNPs are illustrated in Figure 6. The manufactured adsorbents can be easily separated completely by use of an external permanent

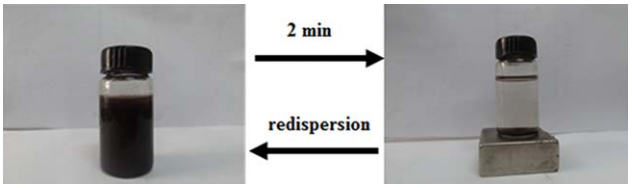

Figure 6. Dispersibility and magnetic sensitivity of DETA-MNPs in an external magnetic field. [Color figure can be viewed in the online issue, which is available at wileyonlinelibrary.com.]

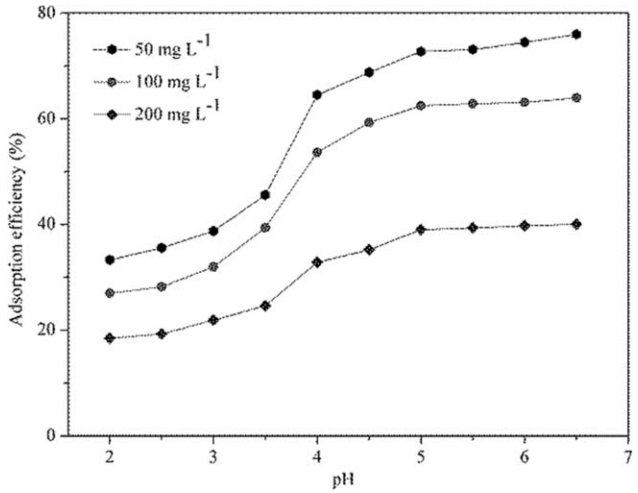

Figure 7. Effect of pH and concentration on Cu(II) adsorption efficiency (%) (adsorbent dosage = 50 mg; pH = 2.0–6.5; V = 50 mL; T = 25°C; contact time = 100 min).

magnet. When the magnet is removed, the nanoparticles would redisperse into the aqueous solution. It's believed that the high magnetic sensitivity and dispersibility play an important role in the adsorption process.

Adsorption of Cu(II)

The influence of the initial solution pH and Cu(II) concentration on the adsorption efficiency is displayed in Figure 7. As was shown, the adsorption efficiency decreases as the initial concentration of Cu(II) grows. The possible explanation is that the available adsorption sites on the surface of the DETA-MNPs are limited. In addition, it is observed that the initial solution pH has strong influence on the adsorption efficiency. The Cu(II) adsorption efficiency rises from 47.51 to 99.94%, 38.53 to 91.37%, 26.32 to 57.18% with the pH varying from 2.0 to 6.5 when the initial Cu(II) concentration is 50, 100, and 200 mg L^{-1}, respectively.

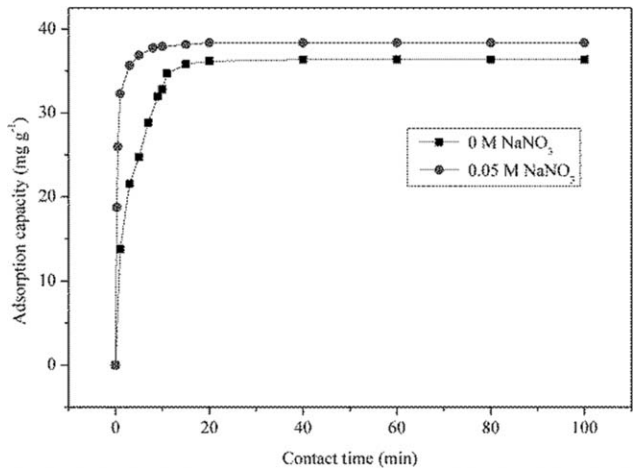

Figure 8. Effect of solution ionic strength on Cu(II) adsorption adjusted by $NaNO_3$ (Cu(II) = 50 mg L^{-1}; adsorbent dosage = 50 mg; pH = 5.0; V = 50 mL; T = 25°C; contact time = 0–100 min).

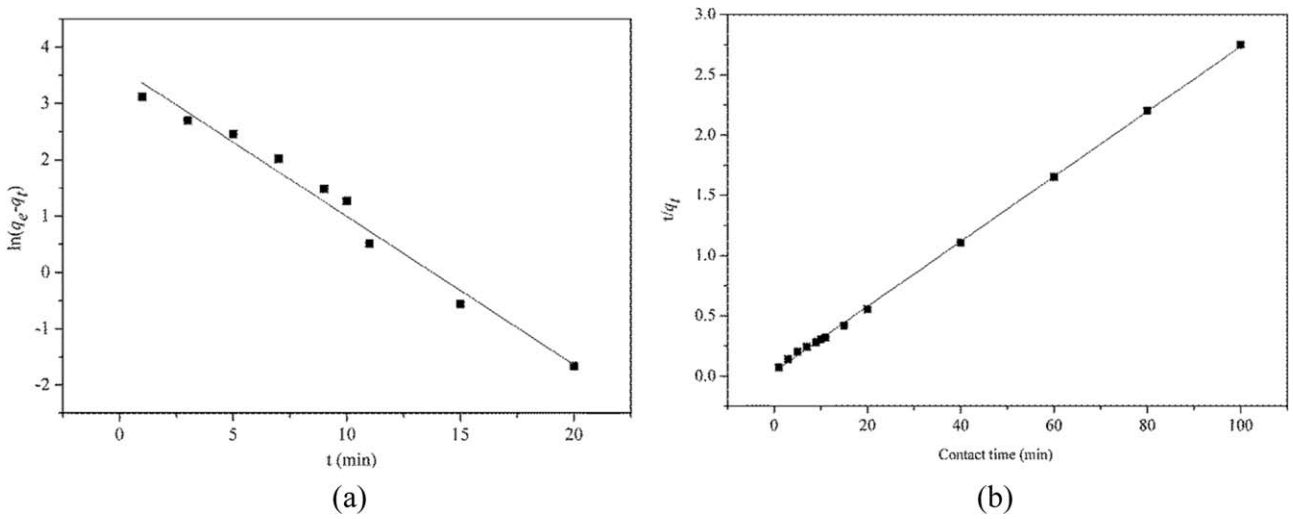

Figure 9. Plots of (a) pseudo-first-order and (b) pseudo-second-order kinetics of Cu(II) adsorption onto DETA-MNPs (Cu(II) = 50 mg L^{-1}; adsorbent dosage = 50 mg; pH = 5.0; V = 50 mL; T = 25°C; contact time = 100 min).

The adsorption efficiency rises sharply in the pH range of 2.0–5.0 and reaches a plateau at pH 5.0. The high pH dependency of the Cu(II) adsorption process may be due to that pH affects not only the surface charges of the adsorbents but also the forms of Cu(II) species.[39] The following equations briefly explain the phenomenon:

$$-NH_2 + H^+ \rightleftharpoons -NH_3^+ \quad (3)$$

$$-NH_2 + Cu^{2+} \rightleftharpoons -NH_2Cu^{2+} \text{ or } -NH_2Cu^{2+}NH_2- \quad (4)$$

Equation (3) presents the reversible protonation/deprotonation process of the amino groups on the surface of DETA-MNPs in solution while eq. (4) illustrates that the amine groups adsorb Cu(II) ions via chelation. When the solution pH < 2.0, a high concentration of H^+ leads to a large quantity of protonated amino groups, which further results in poor adsorption performance due to the weak chelation, and strong electrostatic repulsion between the adsorbents and the positively charged adsorbates.[25] On the other hand, the deprotonation of amino groups accelerates with an increase in pH. At the same time, the electrostatic repulsion between DETA-MNPs and Cu(II) ions gets weaker, which thereby results in a higher adsorption capacity of Cu(II). At pH > 5.0, the adsorption of Cu(II) ions may slightly attribute to the precipitation of $Cu(OH)_2$ ($K_{sp} = 2.2 \times 10^{-20}$). Therefore, the subsequent experiments were carried out at pH = 5.0 to reflect the adsorption performance of DETA-MNPs.

Effect of Solution Ionic Strength

The curves of the adsorption capacity of Cu(II) versus the contact time with different ionic strength using DETA-MNPs as adsorbents are presented in Figure 8. As shown in the figure, the adsorption capacity of Cu(II) increases from 36.36 to 38.35 mg g^{-1} and the adsorption becomes faster with the concentration of $NaNO_3$ increases from 0 to 0.05*M*. Similar results are reported previously by Liu *et al.*[40] Electric double layer is formed on the surface of the particles and the higher the solution ionic strength is, the thinner the electric double layer is, which is in favor of the adsorption process. As the concentration of $NaNO_3$ increases from 0 to 0.05*M*, the electric double layer formed on the particle surface becomes thinner, resulting in a decreased Zeta potential of the particles, which implies the DETA-MNPs are less positively charged. Thus, the surface interaction between the particles and Cu(II) which is also positively charged gets less repulsive. As a result, the addition of $NaNO_3$ enhances and speeds the adsorption.

Kinetics Studies

As shown in Figure 8, the adsorption process is rapid within the first 10 min and reaches equilibrium in 20 min. A shorter adsorption equilibrium time means greater possibility to meet different needs and more economical.

The pseudo-first-order kinetic model and the pseudo-second-order kinetic model are applied to fit the experimental data. The pseudo-first-order kinetic model[1] is expressed as follows:

$$\ln(q_e - q_t) = \ln q_e - k_1 t \quad (5)$$

where k_1 (min^{-1}) is the pseudo-first-order rate constant of adsorption. q_t (mg g^{-1}) and q_e (mg g^{-1}) are the amounts of Cu(II) adsorbed at time t (min) and equilibrium, respectively.

Table I. Kinetic Parameters of Cu(II) Adsorption onto DETA-MNPs

Kinetic model	$q_{e,exp}$ (mg g^{-1})	$q_{e,cal}$ (mg g^{-1})	k_1 (min^{-1})	k_2 (g (mg $min^{-1})^{-1}$)	R^2
Pseudo-first-order	36.36	37.32	0.26	-	0.9844
Pseudo-second-order	36.36	37.08	-	0.02	0.9999

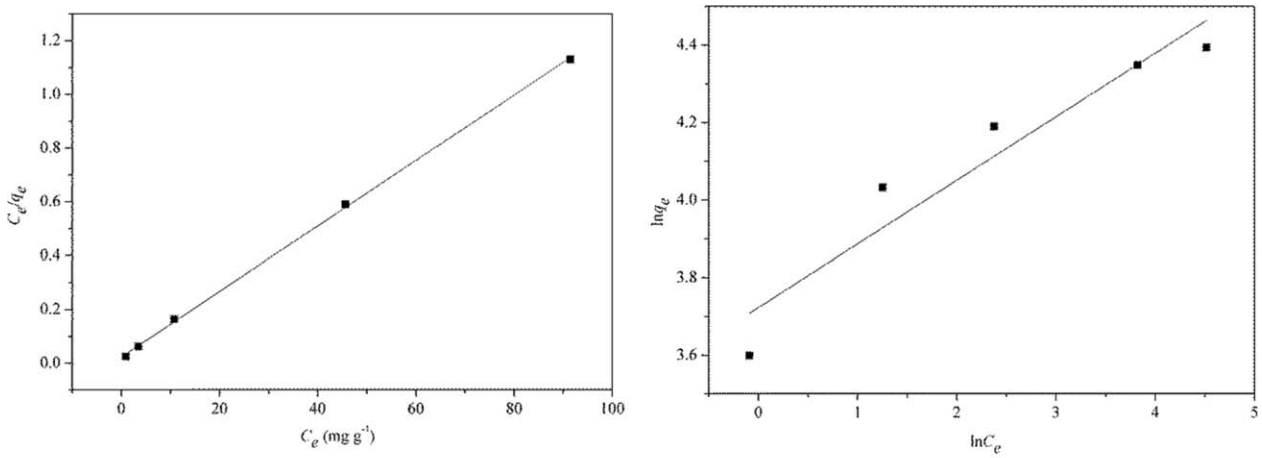

Figure 10. Plots of (a) Langmuir and (b) Freundlich isotherm models for Cu(II) adsorption onto DETA-MNPs (Cu(II) = 50–200 mg L^{-1}; adsorbent dosage: 50 mg; pH = 5.0; V = 50 mL; T = 25°C; contact time = 100 min).

The pseudo-second-order kinetic model[37] is expressed as follows:

$$\frac{t}{q_t} = \frac{1}{k_2 q_e^2} + \left(\frac{1}{q_e}\right) t \tag{6}$$

where k_2 (g (mg $min^{-1})^{-1}$) is the pseudo-second-order rate constant of adsorption. The linear plots of (a) pseudo-first-order kinetic model and (b) pseudo-second-order kinetic model are shown in Figure 9. According to the correlation coefficient (R^2), the pseudo-second-order model [Figure 9(b)] fits the experimental data better than the pseudo-first-order model [Figure 9(a)], which indicates that the adsorption process is controlled by chemisorption involving binding forces through sharing or exchange of electrons between Cu(II) and the amino groups on the surface of DETA-MNPs.[36] The obtained parameters are listed in Table I.

Adsorption Isotherms

The adsorption isotherm is of great significance in estimating the maximum adsorption capacity of the adsorbents. The obtained data are fitted with both Langmuir and Freundlich adsorption models, which assume that the adsorption of Cu(II) occurs on a homogeneous and heterogeneous surface respectively, and the results are shown in Figure 10. The Langmuir adsorption equation[21] is presented as follows:

$$\frac{c_e}{q_e} = \frac{1}{K_L \cdot q_m} + \frac{1}{q_m} \cdot C_e \tag{7}$$

where q_e (mg g^{-1}) and c_e (mg L^{-1}) are the equilibrium adsorption capacity and equilibrium concentration in the aqueous phase; K_L (L mg^{-1}) is the Langmuir equilibrium constant related to adsorption energy and q_m (mg g^{-1}) is the maximum adsorption capacity.

Table II. Langmuir and Freundlich Parameters for Adsorption of Cu(II) onto DETA-MNPs

	Langmuir model			Freundlich model		
	q_m (mg g^{-1})	K_L (L mg^{-1})	R^2	n	K_F (mg g^{-1})(L $mg^{-1})^{1/n}$	R^2
DETA-MNPs	83.33	0.52	0.9995	6.09	41.39	0.8909

Table III. Maximum Adsorption Capacity of Different Magnetic Nanoparticles for Cu(II) Removal

Adsorbent	Equilibrium time (min)	Temperature (°C)	pH	q_m (mg g^{-1})	References
PDA24h-zeolite	1440	25	5.5	28.58	1
PVI/SiO_2	190	25	6	49.2	7
HPIBY	30	20	4.5	19.53	14
Fe_3O_4@PAA@TSC MNPs	45	25	5.0	67.1	15
$NH_2/SiO_2/Fe_3O_4$	120	25	5.5	10.41	37
Chitosan-8-hydroxyquinoline beads	240	28 ± 2	5.0	85.3	41
Diethylenetriamine-bacterial cellulose	120	25	4.5	63.09	42
DETA-MNPs	20	25	5.0	83.33	This study

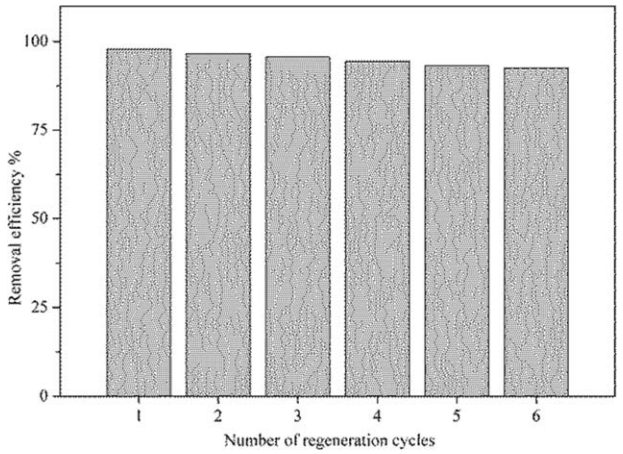

Figure 11. Reusability studies of DETA-MNPs for adsorption of Cu(II).

The Freundlich adsorption model[16] is expressed as follows:

$$\ln q_e = \ln K_F + \left(\frac{1}{n}\right) \ln C_e \tag{8}$$

where K_F (mg g^{-1})(L $mg^{-1})^{1/n}$ is the Freundlich constant related to the adsorption capacity and n is the heterogeneity factor. q_m, K_L and K_F are obtained from the intercept and slope of the linear line by plotting c_e versus c_e/q_e [eq. (7)] and $\log q_e$ versus $\log C_e$ [eq. (8)]. The calculated parameters as well as the correlation coefficients (R^2) are shown in Table II. The adsorption isotherm data fit the Langmuir adsorption model better than the Freundlich model based on R^2, which demonstrates the homogeneous distribution of adsorptive sites on DETA-MNPs and monolayer adsorption of Cu(II).

In addition, a dimensionless constant separation factor (R_L) has commonly applied to predict whether the Langmuir adsorption isotherm is favorable or not, which is defined as follows:[12]

$$R_L = \frac{1}{K_L C_o} \tag{9}$$

where C_o (mg L^{-1}) is the initial concentration of Cu(II), K_L (L mg^{-1}) is the Langmuir isotherm model constant and R_L is the dimensionless Langmuir separation factor. The isotherms are favorable only when R_L is between 0 and 1.[12] In this work, the R_L values are in the range of 0.00637 to 0.037 with Cu(II) concentrations varying from 50 to 200 mg L^{-1}, which implies the adsorption is favorable.

The adsorption capacity of DETA-MNPs under the optimal conditions (Cu(II) concentration = 200 mg L^{-1}, initial solution pH = 5.0, adsorption temperature = 25°C, adsorbent dosage = 50 mg, the volume of adsorption solution = 50 mL, adsorption equilibrium time = 20 min) reaches 79.98 mg g^{-1} and the maximum adsorption capacity calculated from the Langmuir model is 83.33 mg g^{-1}, which is relatively high in comparison with other adsorbents for Cu(II) removal and has a potential use for Cu(II) removal from wastewater. The maximum adsorption capacity (q_m, mg g^{-1}) and the optimal conditions of some adsorbents for Cu(II) removal are presented in Table III.

Regeneration and Reusability

Reusability is of significance when it comes to practical application. To examine the regeneration and reusability of the DETA-MNPs, consecutive adsorption/desorption cycles were repeated six times using 0.1*M* HNO_3, the results are shown in Figure 11. It is found that the adsorption capacity of the DETA-MNPs lowered slightly after each cycle (97.81, 96.58, 95.62 94.39, 93.18, and 92.5%), which is possibly due to a small quantity of Cu(II) irreversibly immobilized onto the surface of the adsorbents. The removal efficiency of Cu(II) remains 92.5% even in the sixth cycle, which implies the DETA-MNPs possess excellent reusability.

CONCLUSIONS

In this work, an amino-functionalized superparamagnetic nanoadsorbent was successfully synthesized via SI-ATRP and subsequent amination reactions and characterized by various techniques, including FT-IR, XRD, TEM, and VSM. The DETA-MNPs can be well dispersed in aqueous solutions with an average diameter of 10 nm. Batch adsorption experiments are carried out to investigate the effects of pH, Cu(II) concentrations, solution ionic strength, and contact time on the adsorption efficiency. It is found that the maximum adsorption capacity of DETA-MNPs is 83.33 mg g^{-1} under the optimal conditions by Langmuir model. The adsorption process depends closely on pH and reaches equilibrium within 20 min. The increasing solution ionic strength can improve the adsorption capacity and shorten the adsorption equilibrium time. The pseudo-second-order kinetic model and the Langmuir isotherm model match the experimental data better. What's more, the fabricated materials exhibit excellent reusability. In conclusion, DETA-MNPs with abundant amino groups are expected to be a promising adsorbent for the Cu(II) removal from wastewater.

REFERENCES

1. Yu, Y.; Shapter, J. G.; Popelka-Filcoff, R.; Bennett, J. W.; Ellis, A. V. *J. Hazard. Mater.* **2014**, *273*, 174.
2. Ahmad, A.; Rafatullah, M.; Sulaiman, O.; Ibrahim, M. H.; Chii, Y. Y.; Siddique, B. M. *Desalination* **2009**, *247*, 636.
3. Cui, L. M.; Wang, Y. G.; Gao, L.; Hu, L. H.; Yan, L. G.; Wei, Q.; Du, B. *Chem. Eng. J.* **2015**, *281*, 1.
4. Fu, L. C.; Liu, F. Q.; Ma, Y.; Tao, X. W.; Ling, C.; Li, A. M.; Shuang, C. D.; Li, Y. *Chem. Eng. J.* **2015**, *263*, 83.
5. Agrawal, A.; Manoj, M. K.; Kumari, S.; Bagchi, D.; Kumar, V.; Pandey, B. D. *Miner. Eng.* **2008**, *21*, 1126.
6. Zheng, Y.; Gao, X. L.; Wang, X. Y.; Li, Z. K.; Wang, Y. H.; Gao, C. J. *RSC Adv.* **2015**, *5*, 19807.
7. Wang, R. X.; Men, J. J.; Gao, B. J. *Clean Soil Air Water.* **2012**, *40*, 278.
8. Huang, B.; Li, Z. W.; Huang, J. Q.; Guo, L.; Nie, X. D.; Wang, Y.; Zhang, Y.; Zeng, G. M. *J. Hazard. Mater.* **2014**, *264*, 176.
9. Chen, Q. Y.; Luo, Z.; Hills, C.; Xue, G.; Tyrer, M. *Water Res.* **2009**, *43*, 2605.
10. Alslaibi, T. M.; Abustan, I.; Ahmad, M. A.; Foul, A. A. *Environ. Prog. Sustain.* **2014**, *33*, 1074.

11. Musso, T. B.; Parolo, M. E.; Pettinari, G.; Francisca, F. M. *J. Environ. Manage.* **2014**, *146*, 50.
12. Komy, Z. R.; Shaker, A. M.; Heggy, S. E. M.; El-Sayed, M. E. A. *Chemosphere* **2014**, *99*, 117.
13. Areco, M. M.; Hanela, S.; Duran, J.; Afonso, M. S. *J. Hazard. Mater.* **2012**, *213/214*, 123.
14. Stanescu, A. M.; Stoica, L.; Constantin, C.; Lacatusu, L.; Oprea, O.; Miculescu, F. *Clean Soil Air Water.* **2014**, *42*, 1632.
15. Zargoosh, K.; Zilouei, H.; Mohammadi, M. Z.; Abedimi, H. *Clean Soil Air Water.* **2014**, *42*, 1208.
16. Ballav, N.; Choi, H. J.; Mishra, S. B.; Maity, A. *J. Ind. Eng. Chem.* **2014**, *20*, 4085.
17. Shen, H. Y.; Pan, S. D.; Zhang, Y.; Huang, X. L.; Gong, H. X. *Chem. Eng. J.* **2012**, *183*, 180.
18. Hu, X. J.; Liu, Y. G.; Zeng, G. M.; Wang, H.; You, S. H.; Hu, X.; Tan, X. F.; Chen, A. W.; Guo, F. Y. *Chemosphere* **2015**, *127*, 35.
19. Peng, W.; Xie, Z. Z.; Cheng, G.; Shi, L.; Zhang, Y. B. *J. Hazard. Mater.* **2015**, *294*, 9.
20. Araghi, S. H.; Entezari, M. H. *Appl. Surf. Sci.* **2015**, *333*, 68.
21. Hao, Y. M.; Chen, M..; Hu, Z. B. *J. Hazard. Mater.* **2010**, *184*, 392.
22. Liu, Y.; Chen, M.; Hao, Y. M. *Chem. Eng. J.* **2013**, *218*, 46.
23. Zhao, F. P.; Repo, E.; Sillanpää, M.; Meng, Y.; Yin, D.; Tang, W. T. *Ind. Eng. Chem. Res.* **2015**, *54*, 1271.
24. Zhang, X. Y.; Huang, Q.; Liu, M. Y.; Tian, J. W.; Zeng, G. J.; Li, Z. L.; Wang, K.; Zhang, Q. S.; Wan, Q.; Deng, F. J.; Wei, Y. *Appl. Surf. Sci.* **2015**, *343*, 19.
25. Xing, H. T.; Chen, J. H.; Sun, X.; Huang, Y. H.; Su, Z. B.; Hu, S. R.; Weng, W.; Li, S. X.; Guo, H. X.; Wu, W. B.; He, Y. S.; Li, F. M.; Huang, Y. *Chem. Eng. J.* **2015**, *263*, 280.
26. Lü, H. X.; Wang, X. M.; Yang, J. Q.; Xie, Z. H. *Int. J. Biol. Macromol.* **2015**, *78*, 209.
27. Li, M. C.; Lee, J. W.; Cho, U. R. *J. Appl. Polym. Sci.* **2012**, *125*, 405.
28. Li, M. C.; Ge, X.; Cho, U. R. *Macromol. Res.* **2013**, *21*, 519.
29. Matyjaszewski, K. *Macromolecules* **2012**, *45*, 4015.
30. Liu, J. L.; He, W. W.; Zhang, L. F.; Zhang, Z. B.; Zhu, J.; Yuan, L.; Chen, H.; Cheng, Z. P.; Zhu, X. L. *Langmuir* **2011**, *27*, 12684.
31. An, F. GB/T 1677-2008; Standards Press of China: Beijing, **2008**.
32. Sidney, S. Quantitative Organic Analysis, 3rd ed.; Wiley: New York, **1967**.
33. Xi, D. L.; Ding, S. X.; Jiang, P. H. HJ/T 27-1999; China Environmental Science Press: Beijing, **2004**.
34. Hu, F. X.; Neoh, K. G.; Cen, L.; Kang, E. T. *Biomacromolecules* **2006**, *7*, 809.
35. Kusvuran, E.; Yildirim, D.; Samil, A.; Gulnza, O. *Clean Soil Air Water* **2012**, *00*, 1.
36. Zhao, Y. G.; Shen, H. Y.; Pan, S. D.; Hu, M. Q.; Xia, Q. H. *J. Mater. Sci.* **2010**, *45*, 5291.
37. Lin, Y. F.; Chen, H. W.; Lin, K. L.; Chen, B. Y.; Chiou, C. S. *J. Environ. Sci.* **2011**, *23*, 44.
38. Bhaumik, M.; Maity, A.; Srinivasu, V. V.; Onyango, M. S. *J. Hazard. Mater.* **2011**, *190*, 381.
39. Tang, Y. C.; Ma, Q. L.; Luo, Y. F.; Zhai, L.; Che, Y. J.; Meng, F. J. *J. Appl. Polym. Sci.* **2013**, *10*, 1799.
40. Liu, C. K.; Bai, R. B.; Hong, L. *J. Colloid Interface Sci.* **2006**, *303*, 99.
41. Barros, F. C. F.; Sousa, F. W.; Cavalcante, R. M.; Carvalho, T. V.; Dias, F. S.; Queiroz, D. C.; Vasconcellos, L. C. G.; Nascimento, R. F. *Clean Soil Air Water* **2008**, *36*, 292.
42. Shen, W.; Chen, S. Y.; Shi, S. K.; Li, X.; Zhang, X.; Hu, W. L.; Wang, H. P. *Carbohydr. Polym.* **2009**, *75*, 110.